

Physical chemical and thermoanalytical characterization of cements based on synthetic hydroxyapatite

Gastón Fuentes Estévez, María Luisa Rojas Cervantes,* José Ángel Delgado García-Menocal, Julio César Llópiz Yurell and Eduardo Peón Avés.**

Biomaterials Center, University of Havana, P.O. Box 6130, Postal Code 10600, Havana, Cuba. Email: gastonfe@biomat.uh.cu.

*Dept. of Inorganic and Technical Chemistry, Faculty of Sciences, UNED, Madrid 28040, Spain. **Institute of Materials and Reactives, University of Havana, Postal Code 10400, Havana, Cuba.

Recibido: 22 de agosto de 2003. Aceptado: 25 de septiembre de 2004.

Palabras clave: hidroxiapatita, cementos, biomaterial, caracterización.

Key words: hydroxyapatite, cement, biomaterial, characterization.

RESUMEN. Se reporta la síntesis y caracterización de cementos basados en hidroxiapatita. Los cementos fueron preparados mezclando una fase sólida formada por hidroxiapatita, yeso, alginato de sodio y *N*-polivinil-2-pirrolidona con una fase líquida que contenía sulfato y fosfato de potasio. Los cementos y sus componentes mayoritarios fueron caracterizados por diferentes técnicas. Las intensidades relativas en los espectros FTIR de las bandas asignadas a los grupos PO_4^{3-} y al agua, cambian con la composición del cemento. Los espectros infrarrojos de los cementos también indican una reducción del grado de cristalinidad de la hidroxiapatita durante la formación del cemento, confirmada por los resultados de RX y la aparición de nuevas bandas asignadas al modo de vibración de grupos carboxilatos como resultado de los polímeros empleados. El comportamiento térmico de los cementos se ve también alterado por la composición de los cementos.

ABSTRACT. The synthesis and characterization of cements based on hydroxyapatite are reported. The cements were prepared by mixing a solid phase formed by hydroxyapatite (HAP), gypsum, sodium alginate (NaAlg) and *N,N*-poly-vinyl-pyrrolidone with a liquid phase containing potassium sulfate and potassium phosphate. The samples so prepared as well as the major components (hydroxyapatite and gypsum) were characterized by x-ray diffraction (XRD), Fourier transform infrared spectroscopy (FTIR), thermogravimetric and differential thermal analysis. The cements so prepared, as well as the major components (hydroxyapatite and gypsum) were characterized by different techniques. The results of FTIR and XRD confirm the high purity and crystallinity of the HAP synthesized and used as raw material for the synthesis of the cements. The relative intensities in the FTIR spectra of the bands assigned to PO_4^{3-} groups and water change with the composition of the cement. FTIR of cements also indicate a reduction in the crystallinity degree of the HAP during the cement formation, confirmed by XRD results, and the appear of new bands assigned to the vibration mode of carboxylate groups from the polymers used. The thermal behaviour of the cements is also affected by the composition of the cements.

INTRODUCTION

Calcium hydroxyapatite is well known $[\text{Ca}_{10}(\text{PO}_4)_6(\text{OH})_2]$ as the primary constituent of bone and teeth of animal organisms.^{1,2} Over the last few years much effort has been made to develop some synthetic and novel materials derived from bone to be used in clinic applications involving bone repair and replacement.³ The most promising and best tolerated of these materials are the cements of calcium phosphate, which can be applied *in situ* in the form of pastes,⁴ due to their great moulding and their adaptability to the shape of the defect. These materials have been extensively used due to their excellent biocompatibility for healthy and rapid tissue growth,⁵ because they are chemically similar to the mineral component of bone tissue and the teeth of animal organisms. Apatite implants are slowly dissolved in the body releasing calcium ions and phosphates that are used by the organism for the growing bone. As the implant is porous, it is gradually filled with bone tissue and is not rejected. Although they show some disadvantages related to the manipulation and their mechanical properties, which have restricted their use as load-bearing implants,^{6,7} they offer a perfect integrity of the bone into the organism. Additionally, they can be applied as a matrix with different incorporated drugs, specially antibiotics, in order to

achieve a controlled liberation of these after the implant has been carried out.⁸

The reasons above mentioned led us to study the preparation of new materials of cements based on hydroxyapatite, capable of removing some undesirable properties of these materials used actually as implants, as the toxicity by monomeric remains and the generation of heat during the setting process, which causes the necrosis of the adjacent tissue.^{9,10} Other desirable properties of these materials are good moulding, easy manipulation and ability to liberate antibiotic in a dosage way at the implant site.^{9,12} As the composition can influence over delivery ability of the material, a good characterization of the cements synthesized is necessary. Therefore, in this paper it is reported the synthesis and characterization of nine cements with different compositions, the effect of the controlled liberation of the antibiotic in the organism being studied in other one.¹³

MATERIALS AND METHODS

Synthesis of the cements

Hydroxyapatite [$\text{Ca}_{10}(\text{PO}_4)_6(\text{OH})_2$] (HAP) and sodium alginate (NaAlg) used for the synthesis of the cements were obtained according to own procedures. In the first case, a solution of phosphoric acid was slowly added under stirring to a suspension containing calcium hydroxide until neutralization, resulting a composition with a Ca/P molar ratio of 1.66. NaAlg is a natural polymer obtained from algae arrivals to the Cuban coasts. Reactants used were: gypsum ($\text{CaSO}_4 \cdot 2\text{H}_2\text{O}$) (Riedel de Haen) and the *N*-poly-vinyl-pirrolidone (PVP) (synthetic polymer of lineal type K90 with an average molecular weight of 360 000) (Merck); potassium sulphate and potassium phosphate (Reachim). All reactants were used as provided.

The cements were synthesized by mixing some components of a solid phase with others in a liquid state. The solid phase is formed by HAP (not sintered and with a size of particle aggregates below the 160 μm), gypsum, NaAlg and PVP. The liquid phase is composed by a solution of K_2SO_4 and K_3PO_4 , which act in the polymerization process as catalyst and delaying agent respectively, in the polymerization process. Different cements were obtained by changing the amounts of the components.

The synthesis scheme of the cements is quite simple. The solid and liquid part were mixed in a plate for

Table 1. Cement compositions.

Cement	Compositions obtained								
	C1	C2	C3	C4	C5	C6	C7	C8	C9
	(wt %)								
HAP	70	70	70	75	75	75	65	65	65
Gypsum	10	15	20	10	15	20	15	20	25
NaAlg	10	7.5	5	7.5	5	2.5	10	7.5	5
PVP	10	7.5	5	7.5	5	2.5	10	7.5	5

one minute approximately. Nine compositions were obtained (Table 1). Although most of the references reported in the literature about cements of hydroxyapatite^{14,15} are based on HAP contents higher than 90 wt%, in our study we have prepared cements with HAP contents between 65 and 75 wt%, because they are values close to that present in human bone (67 wt%).

Characterization techniques

Infrared spectra of raw materials and cements were recorded in a BOMEN DA3 spectrometer in the 4 000-400 cm^{-1} range using the KBr pellet technique. The X-ray powder diffraction patterns were measured and evaluated in the 8-80 2θ range with a Seifert C-3000 diffractometer, using $\text{Cu-K}\alpha$ radiation with a secondary monochromator. Thermogravimetric and differential thermal analyses (TG-DTA) were carried out in a Seiko 55C 5200 TG-DTA 320 system under nitrogen flow of 50 mL/min with a heating rate of 5 $^\circ\text{C}/\text{min}$.

RESULTS AND DISCUSSION

Characterization of hydroxyapatite

The FTIR spectrum and the X-ray diffractogram were obtained for the HAP (Fig. 1). The band centred at 3 574 and the broad band at 3 461 cm^{-1} are assigned to the vibration mode $\nu(\text{OH})$ of adsorbed water or structural hydroxyls. There is another band at 1 629 cm^{-1} , due to the deformation mode H-O-H of water and a double band at 1 449 and 1 418 cm^{-1} , assigned to the carbonate group, which is a possible impurity of the sample caused by the synthesis method. The bands assigned to PO_4^{3-} groups are also observed at 1 093 and 1 041 cm^{-1} (ν_3) and 957 cm^{-1} (ν_1). Additionally, there is a band centred at 871 cm^{-1} , that can be assigned either to the P-OH vibration of the HPO_4^{2-} group or to the carbonate group. These IR results confirm the structure of hydroxyapatite used as raw material in the synthesis of cements.¹⁶⁻¹⁸

The diffraction peaks of the HAP synthesized agree well in d-spacing and relative intensity with those reported in ASTM # 9-432 card (Table 2) and with the obtained by other authors.^{19,20} These data indicate the high purity degree of the HAP used in the synthesis of cements, the impurities detected by IR (water and carbonate) not having an effect on the crystalline structure of the raw material prepared.

Thermoanalysis of the two majority components of the cements (hydroxyapatite and gypsum) were carried out (Fig. 2). In the TG curve of HAP significant weight losses are not observed, but a low and continuous mass loss (ca. 4 wt%) in the complete range of temperature studied.^{21,22} This small loss corresponds to the desorption of adsorbed water (up to 100 $^\circ\text{C}$) and to the removal of part of structural water and hydroxyl ions. On the other hand, the absence of peaks in the DTA curves indicates that the processes implied do not evolve heat change of magnitude enough to be detected by this technique.

These data confirm the fact that the hydroxyapatite is a bioinert material with low thermal degradation.²³ Inversely, in the TG curve of the gypsum a weight loss of around 20 wt% in the 125-150 $^\circ\text{C}$ range is observed, which corresponds almost quantitatively with the loss of two water molecules, as noticed besides in the two well-defined endothermic processes detected in the corresponding DTA curve.

FTIR results

The FTIR spectra of three cements with a constant amount of HAP and variable content of gypsum were obtained (Fig. 3). Some changes are observed in the intensities of the bands with respect to those of pure HAP. First of all, a decreasing of the intensity of the principal bands of PO_4^{3-} groups sited at 1 100 and 1 039 cm^{-1} is observed in the cements spectra.

Additionally, in the cements spectra, a band at 1660 cm^{-1} appears, which

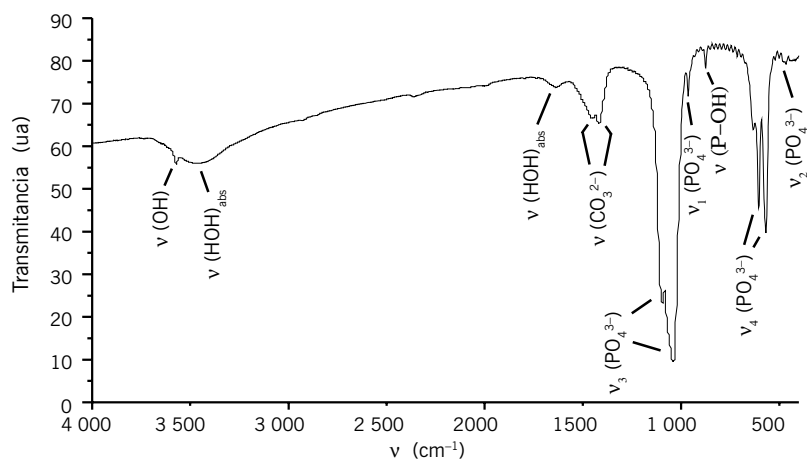


Fig. 1. IR of HAP used as raw material.

Table 2. XRD signals for HAP synthesized and the reported in 9-432 card.

d(Å) HAP	Ir/% HAP	d(Å) 9-432	Ir/% 9-432
3.446	47	3.440	40
2.812	100	2.814	100
2.778	56	2.778	60
2.712	64	2.720	60
2.627	32	2.631	25
2.257	22	2.262	20
1.941	29	1.943	30
1.841	31	1.841	40
1.802	21	1.806	20
1.723	19	1.722	20

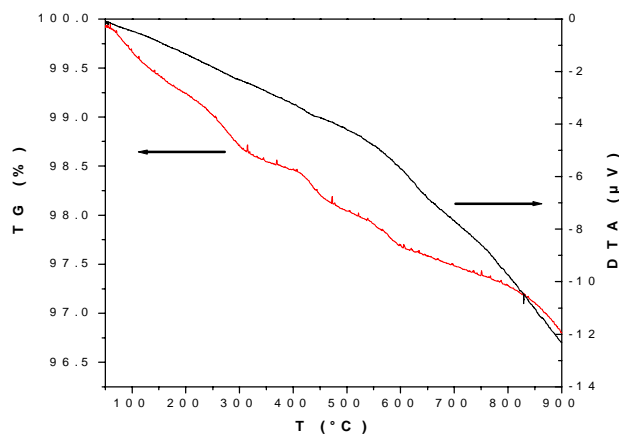


Fig. 2. TG and DTA of the HAP.

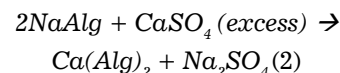
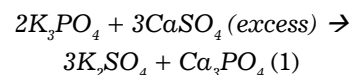
is assigned to the vibration mode of carboxylate group from polymers (NaAlg and PVP). The intensity of the band at 871 cm^{-1} increases significantly in the cements; this band can be assigned to the P-OH vibration of the HPO_4^{2-} groups and also to the vibration of carbonate group, must being the amount of this impurity higher in cements, as corroborated also by the increment of the intensity of the band sited at $1\,640\text{ cm}^{-1}$.

It can be also noticed that the intensity of the bands of PO_4^{3-} centered at $1\,100$ and $1\,039\text{ cm}^{-1}$ is very similar in the three cements spectra, because the amount of HAP is constant. Inversely, the band placed at $3\,400\text{ cm}^{-1}$ assigned to water grows with the gypsum content ($\text{C4} < \text{C5} < \text{C6}$) (Fig. 3). In the same order the intensity of the band at $1\,660\text{ cm}^{-1}$ decreases, because the polymer content also does it when the gypsum

amount increases (Table 1). Notice also the growing of the intensity of the band at $1\,200\text{ cm}^{-1}$ (assigned to SO_4^{2-} groups) with the content of gypsum (this band was absent in the HAP spectrum and (this band was absent in the HAP spectrum and it is almost unappreciable in the spectrum of the sample with less content of gypsum).

It can be noticed the growing in the intensity of bands assigned to PO_4^{3-} groups, and the constancy in the intensity of the bands assigned to water vibrations when increasing the HAP amount ($\text{C7} < \text{C2} < \text{C5}$) (Fig. 4). Inversely, the intensity of the band at $1\,660\text{ cm}^{-1}$ decreases in the order $\text{C7} > \text{C2} > \text{C5}$, because the polymer content does it in this way.

In order to understand some changes produced in the position and intensity of the infrared bands, it is necessary to know the reactions occurring between gypsum and other components, as K_3PO_4 or sodium alginate, defined by the equations 1 and 2:²⁴



The gypsum can react with the K_3PO_4 (which acts as a delaying agent in the setting process), until a complete consumption, as well as with the sodium alginate, a substitution reaction of sodium ions by calcium ions taking over. This last reaction causes the transformation of the alginate from monovalent into divalent salt, occurring a higher crosslinking of the matrix and provoking the setting of the material. The lower covalent character of the Ca-O compared with the Na-O bond causes a shift to a lower wavenumber of the carboxylate vibration if compared with the salts or organic acids (around $1\,680\text{ cm}^{-1}$).²⁵

X-ray diffraction results

Two crystalline phases, HAP and potassium sulfate, were detected in the diffractograms of three selected cements (Fig. 5). This last compound is a product resulting from the setting reaction (Equation 1).

Likewise there is a good agreement (Table 3) between the calculated unit cell parameters and the volumes for both samples (synthesized by us and reported in ASTM).

The values of d-spacing and intensities of X-ray diffraction peaks

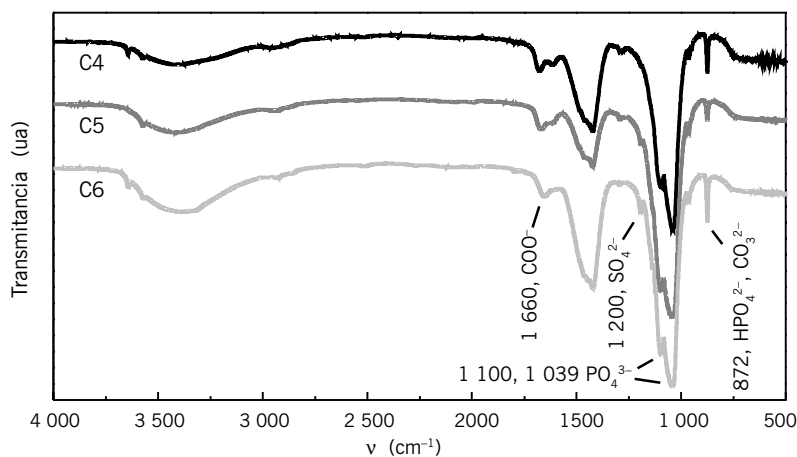


Fig 3. FTIR spectra of cements with variable amount of gypsum.

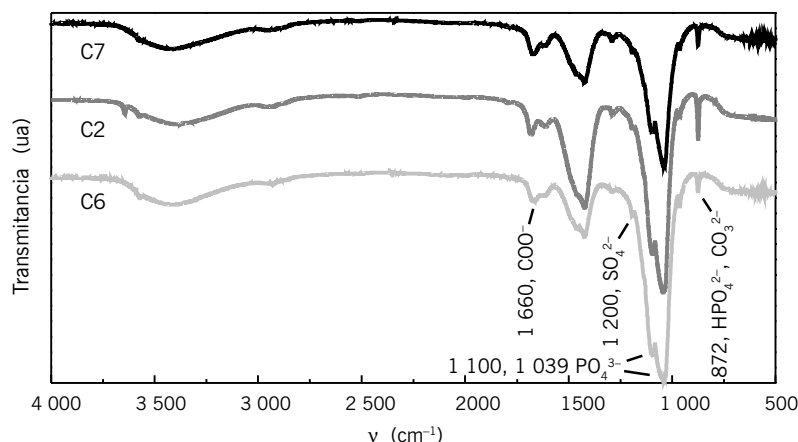


Fig 4. FTIR spectra of cements with variable amount of HAP

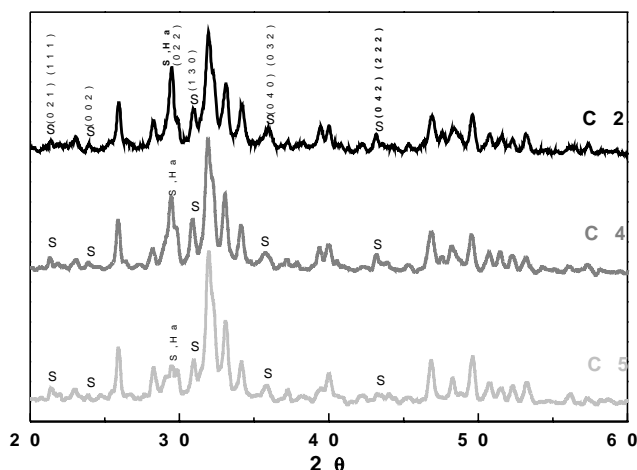


Fig 5. X-ray diffraction patterns of some selected cements. S: K_2SO_4 (5-613 ASTM card). The rest of peaks are assigned to hydroxyapatite. The planes corresponding to the different diffractions are indicated between brackets in the figure.

agree well with those of 9-432 (HAP) and 5-613 (K_2SO_4) cards. In the diffractograms of other cements (C3, C6 and C9, not shown in the figure) containing a higher amount of gypsum, the peaks detected of the sulfate phase are bet-

ter adjusted to the card 15-236 ($K_2S_2O_6$).

It can be noticed a decrease in values of cell-parameters and volume for the HAP when the cements are formed (Table 3). This fact can be due to a light dissolution of the HAP,

produced by the presence of carbonate anions occupying phosphate positions in the network.

The line broadening of the (002) and (202) reflections was used to evaluate the coherence length of the perfect crystalline domains inside the crystals. The d_{hkl} values were calculated from the width at half maximum intensity ($\beta_{1/2}$) using the Scherrer equation (3).²⁶

$$d_{hkl} = \frac{\kappa \cdot \lambda}{\beta_{\frac{1}{2}} \cos \theta} \quad (3)$$

where:

λ the X-ray wavelength.

θ diffraction angle.

κ a constant varying with crystal habit and chosen as 0.9.

The results (Table 4) indicate that the d_{hkl} values of crystallite size of the HAP phase in cements are significantly reduced with respect to those of pure HAP. This loss of crystallinity during the formation of the cements agrees with the results observed by FTIR. Although there is no a clear relation between the HAP content of the cement and the reduction degree of the crystal size, in some cases reduction values of up to 45 % are observed, being greater the reduction in the direction parallel to the *b*-axis. These results confirm the reduction observed in the cell parameters and volume values.

Results of thermal analysis

The residue values of samples after TG analysis are listed in Table 5.

All cements undergo to weight losses varying from 15 to 30 wt%, with the exception of C3 sample, which experiments a weight loss of around 45 wt%. This fact can be due probably to an error in the preparation of this sample, because this cement resulted to contain a water amount much higher than the rest of samples.

All the cements showing a very similar thermal behaviour in TG and DTA curves (Fig. 6). Four well-defined weight losses are differentiated in the TG curve. The first zone up to around 150-170°C can be assigned to the loss of adsorbed water and the hydration water.

There are other three weight losses in the 200-350, 350-600 and 600-750 °C temperature ranges, which can be associated with the pyrolysis of the organic groups of the polymeric additives. The four weight losses observed are associated with four endothermic processes detected in the respective DTA curve (Table 5).

Table 3. Cell parameters of cements and HAP.

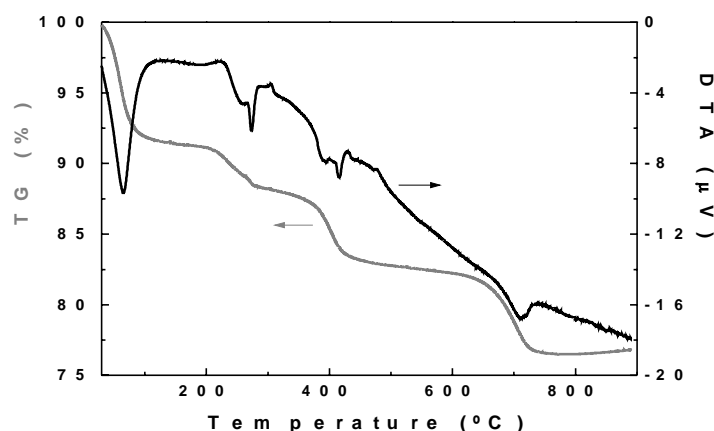
Cement	a = b/Å	c/Å	V/Å ³	Cement	a = b/Å	c/Å	V/Å ³
C1	9.56	6.874	527.8	C7	9.357	6.856	519.8
C2	9.372	6.864	522.1	C8	9.382	6.862	523.1
C3	9.377	6.877	523.7	C9	9.361	6.852	520.0
C4	9.379	6.871	523.4	HAP	9.397	6.892	527.0
C5	9.385	6.864	523.6	9-432	9.418	6.884	528.8
C6	9.377	6.874	523.4				

Table 4. Crystal size of the HAP phase evaluated by Scherrer equation for the (002) and (202) reflections.

Sample	d(002)/Å	d(202)/Å
HAP	338.6	335.6
C1	310.2	236.1
C2	319.1	228.8
C3	202.3	242.3
C4	307.5	216.5
C5	281.8	221.1
C6	282.8	284.5
C7	273.2	214.7
C8	281.6	210.0
C9	313.2	179.1

Table 5. Residue values (wt%) of cements after thermogravimetric analysis and temperature of the minima of the DTA peaks.

Cement	C1	C2	C3	C4	C5	C6	C7	C8	C9
Residue (wt%)	69.5	77.8	55.3	78.8	83.6	85.1	74.7	76.5	79.8
	65.1	63.4	89.7	62.7	58.9	62.4	60.2	65.2	64.2
Temperature (°C)	245.4	276.4	256.9	244.7	273.3	275.5	272.1	274.0	275.0
	410.9	402.6	412.8	407.1	406.4	391.9	414.7	415.5	403.0
	717.3	726.5	708.4	712.6	694.0	726.8	700.2	710.8	740.4


Fig. 6. Thermal analyses of C8 cement.

It can be observed that the higher the content of HAP the higher the final residue is, that is, the lower the

weight loss (Fig. 7). Considering that the HAP used as raw material for the synthesis of the cements shows a

very low weight loss in the studied temperature range (Fig. 3), the differences observed in the values of the remains of these samples can be attributed to the different amounts of NaAlg and PVP used for the synthesis. Thus, the C7 sample is the one of the three cements shown that contains a higher amount of these two components, therefore showing the highest weight loss.

The contribution to the total weight loss is the addition of the mass loss due to the potassium sulfate and that one associated with the decomposition polymers (Fig. 8). It can be observed that when the gypsum amount increases, the residue value also does it, that is, the weight loss decreases. This can be explained by attributing the different losses to the polymerizing agents (NaAlg and PVP) whose molecular weights are much higher than that of potassium sulfate. Thus, when the amount of gypsum in the cement composition increases, the amount of the organic additives decreases, therefore diminishing the weight loss. The same trend is observed by comparison of the results of thermogravimetric analyses of samples C7, C8 and C9.

CONCLUSIONS

Nine cements with different compositions of HAP, gypsum, NaAlg and PVP have been prepared. The results of FTIR indicate a reduction in the crystallinity degree of the HAP during the cement formation.

The intensity of the bands associated with PO_4^{3-} groups increases with the HAP content of the cement and that of the bands assigned to water does with the gypsum content. New bands assigned to sulphate and carboxylate groups appear in the cements spectra, their intensities increasing with the amount of gypsum and polymer, respectively.

The loss of crystallinity of the HAP in the cements is also confirmed by XRD, being greater in the direction parallel to the baxis. By thermal analysis it is observed that the higher the content of HAP, the lower is the weight loss, being attributable this weight loss principally to the decomposition of the polymers, PVP and NaAlg used in the synthesis of the cements.

These cements can be applied as a matrix with different incorporated drugs, to be liberated in a controlled way at the implant site.

ACKNOWLEDGMENTS

The authors thank the financial support of the project from the Ex-

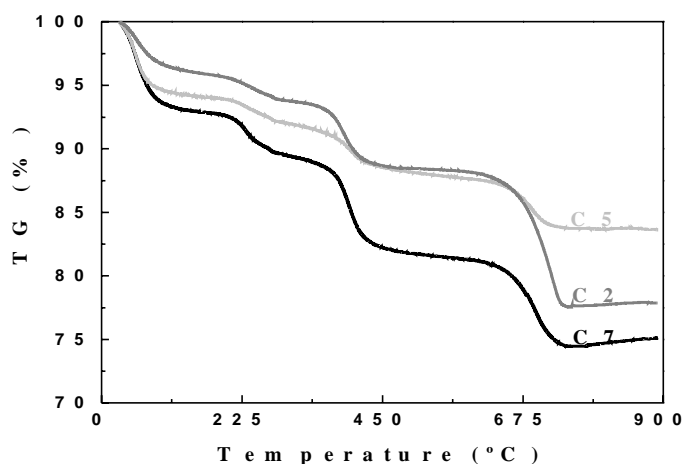


Fig. 7. Thermogravimetric analyses of different cements with variable amount of HAP.

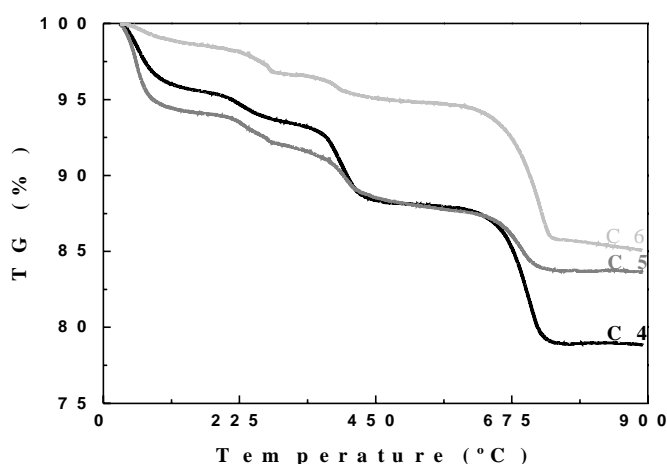


Fig. 8. Thermogravimetric analyses of different cements with variable amount of gypsum.

pert Fund of AECI-ICI "Desarrollo de cementos de HAP como sistemas de liberación controlada de fármacos" between Biomaterials Center of University of Havana, Cuba, and the Department of Inorganic Chemistry of UNED, Spain.

BIBLIOGRAPHY

- Jarcho M., Kay J.F., Gumaer K.I., Doremus R.R. and Drobeck H.P. Tissue, cellular and subcellular events at a bone ceramic hydroxyapatite interface, **J. Bioeng.**, **1**, 79, 1977.
- Katz J.L. and Harper R.A. in Encyclopedia of Materials Science and Engineering, Pergamon Press Eds., New York, Vol. 1, 474, 1986.
- Hollinger J.O., Brekke J., Gruskin E. and Lee D. Role of bone substitutes, **Clin. Orthop.**, **324**, 55, 1996.
- Driessens F.C.M., Boltong M.G., Bermudez O., Planell J.A., Ginebra M.P. and Fernandez E. Effective formulations for the preparation of calcium phosphate bone cements, **J. Mater. Sci.: Mater. Med.**, **5**, 164, 1994.
- Jarcho M., Bolen C.H., Thomas M.B., Bobick J., Kay J.F. and Doremus R.H. Hydroxyapatite synthesis in dense polycrystalline form, **J. Mater. Sci.**, **11**, 2027, 1976.
- Martin R.I. and Brown P.W. Mechanical properties of hydroxyapatite formed at physiological temperature, **J. Mater. Sci.: Mater. Med.**, **6**, 138, 1995.
- Pilliar J.E. Davies and Smith D.C. The bone-biomaterial interface for load-bearing implants. **Mater. Res. Bull.**, **16**, 55, 1991.
- Willmann G.C. Medical grade of hydroxyapatite: state of the art, **British Ceram. Trans.**, **95**, 212, 1996.
- Otsuka M., Matsuda Y., Yu D., Wong J., Fox J.L. and Higuchi W.I. A novel skeletal drug delivery system for anti-bacterial drugs by using self-setting hydroxyapatite cement, **Chem. Pharm. Bull.**, **38**, 3500, 1990.
- Bohner M., Lemaitre J., Van Landjyt P., Zambelli P.Y., Merckle H.P. and Gander B. Hydraulic calcium phosphate bone cement as antibiotic drug delivery system **J. Pharm. Sci.**, **86**, 565, 1997.
- Zuev V.P., Pankratov A.S., Sergeev P.V., Bolotova E.N. and Semeikin A.V. Lincomycin pharmacokinetics during its use as a component of drug composition with ultrahighly dispersed hydroxyapatite, **Clin. Orthop.**, **355**, 238, 1998.
- Yamashita Y., Uchida A., Yamakawa T., Shinto Y., Araki N. and Kato K. Treatment of chronic osteomyelitis using calcium hydroxyapatite ceramic implants impregnated with antibiotic. **Int Orthop.**, **22**, 247, 1998.
- Fuentes G., Rojas M.L., Peón E., García D. and Casquero J. Composition influence on delivery ability of hydroxyapatite cements. **Revista CENIC Ciencias Químicas**, **33**, 7, 2002.
- Ito M. *In vitro* properties of a chitosan-bonded hydroxyapatite bone-filling paste, **Biomaterials**, **12**, 41, 1991.
- Kawakami T., Antoh M., Hasegawa H., Yamagishi T., Ito M. and Eda S. Experimental study on osteoconductive properties of a chitosan-bonded hydroxyapatite self-hardening paste, **Biomaterials**, **13**, 759, 1992.
- Zhong J.P., LaTorre G.P., Hench L.L. The kinetics of bioactive ceramics Part VII: Binding of collagen to hydroxyapatite and bioactive glass, **Bio-ceramics**, **7**, 62, 1994.
- Kandori K., Yasukawa A., Ishikawa T. Preparation and characterization of spherical calcium hydroxyapatite, **Chem. Mater.**, **7**, 26, 1995.
- Fowler B.O. Infrared studies of apatites. I. Vibrational assignments for calcium, strontium, and barium hydroxyapatites utilizing isotopic substitution, **Inorg. Chem.**, **13**, 194, 1974.
- Arends J., Christoffersen J., Christoffersen M.R., Eckert H., Fowler B.O., Heughebaert J.C., Nancollas G.H., Yesinowski J.P. and Zawacki S.J. A calcium hydroxyapatite precipitated from an aqueous solution: An international multimethod analysis. **J. Crystal Growth**, **84**, 515, 1987.
- Van Blitterswijk C.A., Grote J.J., Kuijpers W., Daems W.T. and De Groot K. Macropore tissue ingrowth: a quantitative and qualitative study on hydroxyapatite ceramic, **Biomaterials**, **7**, 137, 1986.
- Toriyama M., Kawamura S., Ito Y. and Nagae H. Thermal change in calcium-deficient apatite obtained by mechanochemical treatment", **J. Ceram. Soc. Jpn.**, **97**, 554, 1989.
- Yang G. and Wang Z. Synthesis of biphasic ceramics of hydroxyapatite and -tricalcium phosphate with controlled phase content and porosity, **J. Mater. Chem.**, **8**, 2233, 1998.
- Tomazic B. and Nancollas G.H. Seeded growth of calcium phosphates. Surface characterization and the effect of seed material, **J. Colloid Interf. Sci.**, **50**, 451, 1975.
- Ishikawa K. and Miyamoto Y. Non decay type fast setting calcium phosphate cement: composite with sodium alginate, **Biomaterials**, **16**, 527, 1995.
- Carey F. in Organic Chemistry, 2nd Ed., McGraw-Hill Eds., 762, 1987.
- Klug H.P. and Alexander L.E. X-Ray Diffraction procedures for Polycrystalline and Amorphous Materials, Chapter 9nd, John Wiley and Sons Eds., New York, 687-704, 1974.